Rotaxanes

DOI: 10.1002/ange.200502624

An Allosterically Regulated Molecular Shuttle**

Dana S. Marlin, Diego González Cabrera, David A. Leigh, and Alexandra M. Z. Slawin*

One of Nature's most effective ways of influencing function from afar is through allosteric control.[1] This occurs—most typically in proteins—when activity at a substrate-binding site is modulated by the complexation of an effector molecule or

[*] Dr. D. S. Marlin, D. González Cabrera, Prof. D. A. Leigh
School of Chemistry
University of Edinburgh
The King's Buildings
West Mains Road
Edinburgh EH9 3JJ (UK)
Fax: (+44) 131-667-9085
E-mail: David.Leigh@ed.ac.uk
Prof. A. M. Z. Slawin
School of Chemistry
University of St. Andrews
Purdie Building
St. Andrews
Fife KY16 9ST (UK)

[**] This work was supported by the European Union Future and Emerging Technology Program Hy3M and the EPSRC. D.S.M. is a Marie Curie Fellow; D.A.L. is an EPSRC Senior Research Fellow and holds a Royal Society–Wolfson Research Merit Award.

Supporting information for this article is available on the WWW under http://www.angewandte.org or from the author.

ion at a second site. The binding sites are frequently several nanometers apart, and communication between them is achieved through a variety of mechanisms, the details of which are not well understood but often involve multiple substrate-binding sites and cooperative complexation events that are accompanied by large amplitude movements of polypeptide chains and other molecular subunits.[2] However, to achieve any kind of distant control in response to binding in synthetic systems is far from trivial. Most of the artificial allosteric receptors developed to date feature one or more substrate-interaction sites directly conformationally coupled to an effector-binding site.[3] Herein, we report on a mechanically linked substrate/host ensemble (a [2]rotaxane), which contains two spatially and chemically distinct "substrate" hydrogen-bonding sites, only one of which is influenced by the coordination of a metal ion (the "effector") to an adjacent tridentate ligand fragment. The result is a stimuli-responsive molecular shuttle[4] that undergoes a large amplitude internal motion (change in the position and binding strength of the macrocycle), allosterically regulated through a small, but highly significant, conformational change brought about by complexation of a transition metal at the effector site.

The molecular shuttle allosteric control mechanism has its origins in anomalous behavior observed for some simple hydrogen-bonded rotaxanes that bear metal-chelating stoppers containing a bis(2-picolyl)amine (BPA)[5] moiety (Scheme 1). Rotaxanes **1** and **2**, in which the BPA unit is connected to the hydrogen-bonding groups of the thread by an ethylene spacer, react readily with various transition-metal salts including $CuCl_2$, which yields complexes **1**$CuCl_2$ and **2**$(CuCl_2)_2$, respectively (Scheme 1a and b). The X-ray crystal structures of **1**$CuCl_2$ and **2**$(CuCl_2)_2$ (Figure 1a and b) show the typical four intercomponent hydrogen bonds between the benzylamide groups of the macrocycle and the amide groups of the thread,[6] together with the predicted coordination of the BPA ligands to each metal ion in a tridentate fashion. However, to our surprise, rotaxanes **3** and **4**, in which the ethylene spacer is absent and the BPA unit is attached directly to the hydrogen-bonding station of the thread, were found *not* to react[7] with $CuCl_2$ or similar transition-metal salts even under forcing conditions (Scheme 1c and d). This behavior is in marked contrast to that of their parent threads, which react like rotaxanes **1** and **2** to give the expected coordination complexes, indicating that the reduced electron density on the nitrogen atom caused by the adjacent carbonyl group is not the reason for the lack of reaction of **3** and **4**.[5]

The X-ray crystal structures of **3** and **4** (Figure 1c–f) reveal the reason for their lack of reactivity. Although the macrocycles in **3** and **4** form hydrogen bonds to the thread through the four intercomponent hydrogen bonds (shown in the stick representation, Figure 1c and d) analogous to rotaxanes **1** and **2**, the pyridine arms of the BPA groups are forced close-to-parallel with the isophthalamide groups of the macrocycle (concomitantly forming favorable π–π-stacking interactions) to accommodate the ring on the hydrogen-bonding site. To chelate to a metal ion by using all three nitrogen atoms of the BPA group, the pyridine arms must twist orthogonally, causing them to enter space that is already occupied by the benzylamide macrocycle. However, the

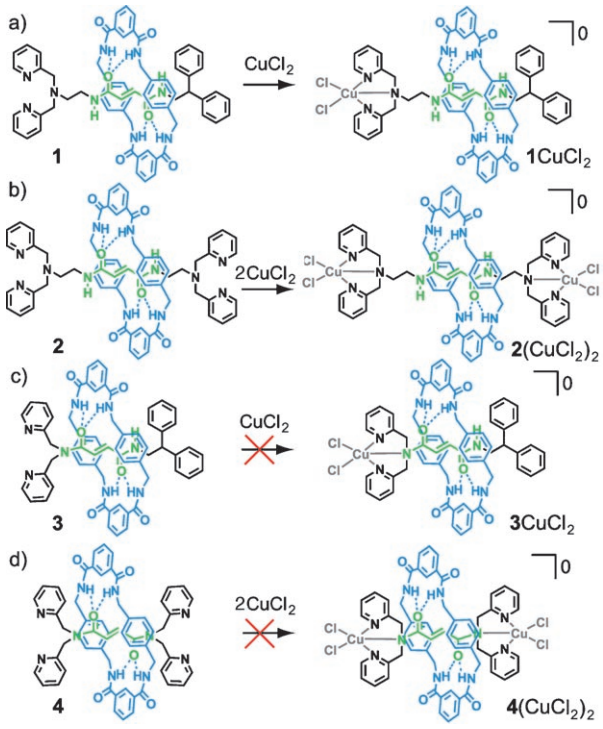

Scheme 1. Rotaxanes **1**–**4** and their attempted complexation reactions with one (a, c) or two (b, d) equivalents of $CuCl_2$ in DMF at room temperature. Complexes **1**$CuCl_2$ and **2**$(CuCl_2)_2$ are formed in near-quantitative yield and were purified by recrystallization from CH_3CN/DMF;[8] **3**$CuCl_2$ and **4**$(CuCl_2)_2$ could not be detected even upon heating at 80 °C for 12 h.[7] The free threads of **1**–**4** each react readily with $CuCl_2$ in DMF at room temperature to form coordination complexes that are analogous to **1**$CuCl_2$ and **2**$(CuCl_2)_2$.

macrocycle physically has nowhere else to move to in either **3** or **4** (see the space-filling representations, Figure 1e and f) and so the conformational change required for the BPA group to chelate to a transition metal cannot take place in these short congested rotaxane structures.

The prospect of a situation where, despite binding at different sites, metal- and macrocycle-binding modes compete for the same 3D space led us to consider whether translocation of the macrocycle to a second hydrogen-bonding site on a thread could be induced by a metal-binding interaction. As a model we designed rotaxane **5** (Scheme 2), which contains three carbonyl hydrogen-bond acceptors on the thread in what can be viewed as an elongated hydrogen-bonding station (for clarity in interpreting the ^{1}H NMR spectra (Figure 2), one half of this unit is colored in green and the other in orange). With this extended station the macrocycle in **5** has space to occupy (and hydrogen-bonding partners) when a metal binds to, and rearranges the conformation of, the BPA-containing stopper. The solid-state structure of **5** (Scheme 2b) reveals that the macrocycle is bound to the central carbonyl group (O41) of the thread through hydrogen bonds between the carboxamide hydrogen donors (N20H and N29H) and the amide carbonyl group adjacent to the diphenylacetyl stopper (O44). However, the carbonyl group (O38) adjacent to the BPA station is also in the plane of the other two carbonyl groups (O41 and O44) on the thread, and in solution one

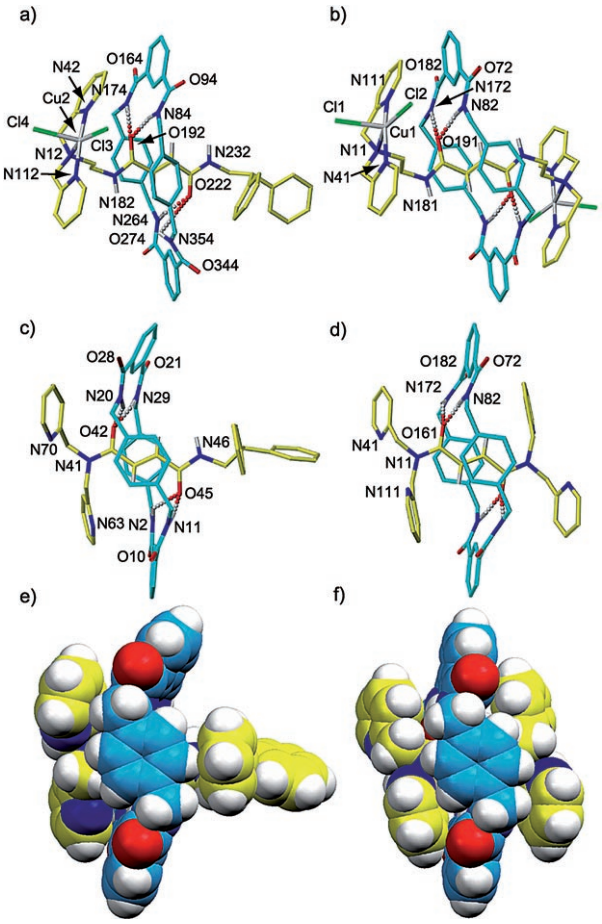

Figure 1. X-ray crystal structures[8] of a) **1**$CuCl_2$, b) **2**$(CuCl_2)_2$, c) **3**, and d) **4** in stick representation, and e) **3** and f) **4** in space-filling van der Waals radius form. C (thread) yellow, C (macrocycle) turquoise, O red, N dark blue, Cu gray, Cl green, H white. In the stick representations, all hydrogen atoms except for the amide and olefin protons have been omitted for clarity. Selected bond lengths [Å]: **1**$CuCl_2$: N12–Cu2 2.075, N42–Cu2 1.987, N112–Cu2 1.987, Cl3–Cu2 2.235, Cl4–Cu2 2.563, N264H–O222 2.236, N354H–O222 2.353, N174H–O192 2.260, N84H–O192 2.290; **2**$(CuCl_2)_2$: N11–Cu1 2.076, N41–Cu1 2.001, N111–Cu1 2.027, Cu1–Cl1 2.497, Cu1–Cl1 2.232, N172H–O191 2.140, N82H–O191 2.260; **3**: N20H–O42 2.239, N29H–O42 2.136, N2H–O45 2.687, N11H–O45 1.957; **4**: N172H–O161 1.985, N82H–O161 2.212.

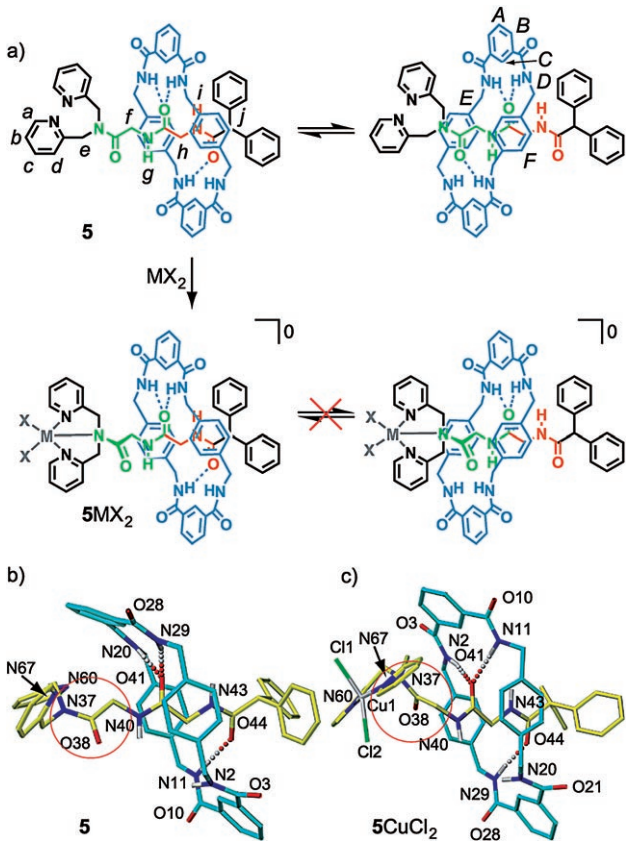

Scheme 2. Synthesis of [2]rotaxane **5** with an extended hydrogen-bonding site and its subsequent complexation to generate **5**MX_2 ($MX_2 = CuCl_2$ or $Cd(NO_3)_2$): a) the solution positional equilibrium of the macrocycle in **5** (atom-lettering scheme corresponds to ^{1}H NMR assignments in Figure 2). The complexes **5**MX_2 were prepared by addition of a solution of the appropriate metal salt in acetonitrile to a solution of **5** in acetonitrile at room temperature and purified by crystallization. b, c) X-ray crystal structures[8] of **5** and **5**$CuCl_2$, respectively. C (thread) yellow, C (macrocycle) turquoise, O red, N dark blue, Cu gray, Cl green, H white; all hydrogen atoms except for the amide protons have been omitted for clarity. Selected bond lengths [Å]: **5**: N20H–O41 2.026, N29H–O41 2.192, N11H–O44 1.888; **5**$CuCl_2$: N37–Cu1 2.432, N60–Cu1 1.976, N67–Cu1 1.987, Cl1–Cu1 2.256, Cl2–Cu1 2.227, N2H–O41 2.190, N11H–O41 2.153, N29H–O44 1.885. The red circles highlight the enforced change in conformation of the BPA ligand and adjacent peptide unit upon coordination to a metal ion.

would expect an equilibrium to exist between the hydrogen bonding of N11H and O44 and a similar interaction between O38 and N2H (Scheme 2a). Indeed, the ^{1}H NMR spectrum of rotaxane **5** in CD_3CN (Figure 2b) reveals that this is the case, with the chemical shifts of both internal methylene groups H_f and H_h (green and orange, respectively) shifted upfield ($\Delta\delta H_f = 0.7$ ppm; $\Delta\delta H_h = 1.0$ ppm) relative to those of the free thread (Figure 2a), as a result of shielding from the macrocycle.

Addition of $CuCl_2$ to **5** results in formation of complex **5**$CuCl_2$, the X-ray crystal structure of which is shown in Scheme 2c. The most striking characteristics of this solid-state structure are the chelation of all three BPA nitrogen atoms (including the carboxamide nitrogen, N71) to the Cu^{II} ion, together with the out-of-plane tilting of carbonyl oxygen O38 relative to the plane in which the other two carbonyl oxygen atoms (O41 and O43) of the thread lie. As cadmium is a diamagnetic metal with similar binding properties to Cu^{II}, treatment of **5** with $Cd(NO_3)_2$ allowed us to study the solution behavior of metal chelation to **5** using ^{1}H NMR spectroscopy (compare Figure 2c with Figure 2b and d). As expected, the binding of a metal ion to the BPA stopper alters the equilibrium of hydrogen bonding between the three carbonyl hydrogen-bond acceptors in **5**, causing a shift of the signal for H_h (orange) further upfield and a slight downfield shift of the resonance for H_f (green) in **5**$Cd(NO_3)_2$ relative to those in the free rotaxane. Comparison of the ^{1}H NMR spectra of **5**$Cd(NO_3)_2$ with the $Cd(NO_3)_2$–thread complex revealed a similar trend, that is, a large upfield shift of the signal for H_h and a much smaller shift for that of H_f. The changes indicate that the

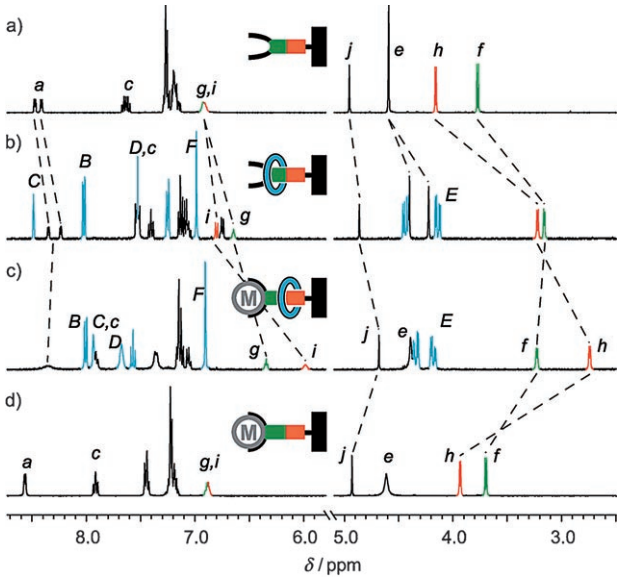

Figure 2. Partial ^{1}H NMR spectra (400 MHz, CD_3CN, 298 K) of a) the thread of rotaxane **5**, b) **5**, c) **5**$Cd(NO_3)_2$, and d) the complex of the thread of rotaxane **5** with $Cd(NO_3)_2$. Resonances are colored and labeled as shown in Scheme 2.

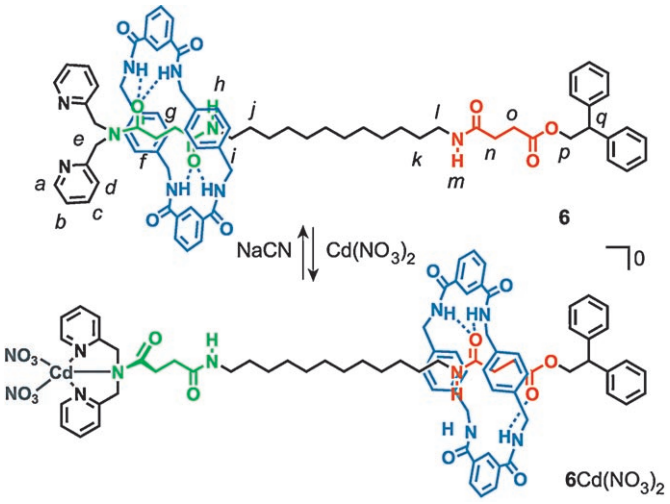

Scheme 3. An allosterically regulated molecular shuttle. Rotaxane **6** consists of a BPA metal-chelating site (the "effector" binding site), two hydrogen-bonding stations of different intrinsic affinities (substrate-binding sites), and a benzylamide macrocycle substrate. Metal complexation of **6** occurs quantitatively at room temperature with $Cd(NO_3)_2$ in CD_3CN. The reverse transformation is accomplished by treatment with excess NaCN (5 equiv).

macrocycle no longer shuttles back and forth along the thread in **5**$Cd(NO_3)_2$ but is restricted mainly to a position over the H_h methylene group between carbonyl oxygen atoms O41 and O43.

Encouraged by the results from this model system we prepared a two-station [2]rotaxane, **6**, with hydrogen-bonding sites of substantially differing affinities[9] for the macrocycle separated by a C_{12} alkyl chain. The station of known[9] higher binding affinity (succinamide, shown in green) is directly attached to the metal-binding BPA unit, while the station of inherent lower affinity[9] (succinic amide ester, shown in orange) is attached to a nonchelating diphenylacetyl stopper (Scheme 3). In **6**, the macrocycle occupies the position over the green station more than 95% of the time at 273 K in CD_3CN, as revealed by the large ($\Delta\delta = 1.5$ ppm) upfield shift of the signals for protons H_f and H_g (compare Figure 3b and a). In comparison, the signals for protons H_n and H_o (orange station) appear at similar chemical shifts in rotaxane **6** (Figure 3a) and the parent thread (Figure 3a).

The addition of one equivalent of $Cd(NO_3)_2$ to **6** in CD_3CN results in a dramatic change in the ^{1}H NMR spectrum (Figure 3c). The major differences in the spectra of **6** and **6**$Cd(NO_3)_2$ are the large ($\Delta\delta = 1.1$ ppm) downfield shift of the signals for protons H_f and H_g (green station) and the upfield shift ($\Delta\delta = 0.7$ ppm) of the peaks for H_n and H_o (orange station) in the metal-coordinated rotaxane. In addition, protons H_l, H_p, and H_q at the periphery of the orange station are also shielded by the macrocycle ($\Delta\delta \approx 0.3$ ppm). Collectively these data indicate that the macrocycle has moved from residing predominantly over the green station to being positioned mainly over the orange station. The difference in the chemical shifts of **6**$Cd(NO_3)_2$ relative to those of the parent thread bound to $Cd(NO_3)_2$ (Figure 3d) confirms the change in position of the macrocycle. The coordination

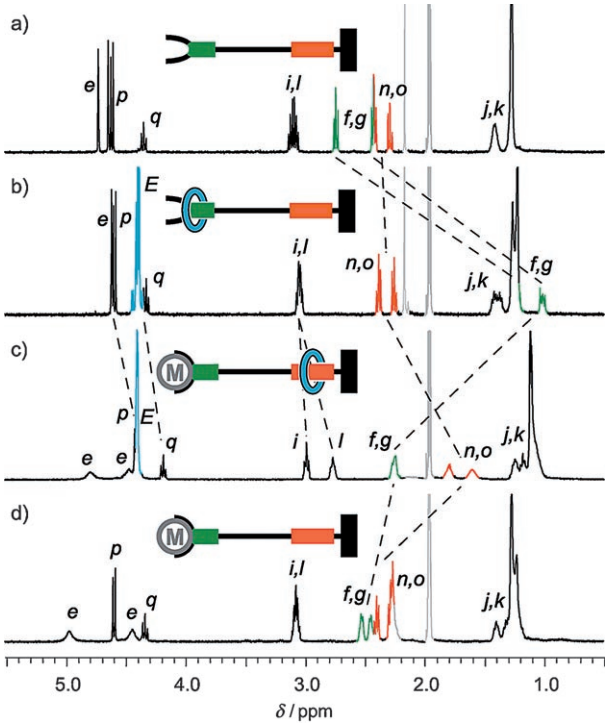

Figure 3. Partial ^{1}H NMR spectra (400 MHz, CD_3CN, 273 K) of a) the parent thread of **6**, b) **6**, c) **6**$Cd(NO_3)_2$, and d) the complex of the parent thread of **6** with $Cd(NO_3)_2$. Resonances are colored and labeled as shown in Scheme 3. Peaks shown in light gray arise from residual non-deuterated solvent and water.

reaction, and change in position of the macrocycle, is reversed by treatment with NaCN (Scheme 3).

The stimuli-induced shuttling between **6** and **6**$Cd(NO_3)_2$ (Scheme 3) corresponds to a negative heterotropic allosteric

binding event[10]—inhibition of hydrogen bonding of the macrocycle at the succinamide unit through the conformational change induced by metal chelation at the BPA site—that leads to translocation of the macrocycle to the inherently weaker hydrogen-bonding succinic amide ester site, which lies 1.5 nm away. Similarly large movements in rotaxanes have been used to bring about changes in conductivity,[4d,11] circular dichroism,[12] fluorescence,[13] porosity,[14] and surface energy,[15] and to carry out mechanical work,[15,16] largely as a result of chemical (redox, acid-base, and photochemical) reactions on the covalent structure of the rotaxane. An allosteric shuttling mechanism offers the possibility of using metal-binding events as the energy source or operating stimulus for functional synthetic molecular machines.

Received: July 26, 2005
Revised: October 1, 2005
Published online: January 30, 2006

Keywords: allosterism · hydrogen bonds · molecular devices · rotaxanes · transition metals

[1] For recent reviews on allostery in biological systems, see: a) J.-P. Changeux, S. J. Edelstein, *Neuron* **1998**, *21*, 959–980; b) R. R. Breaker, *Nature* **2004**, *432*, 838–845; c) J.-P. Changeux, S. J. Edelstein, *Science* **2005**, *308*, 1424–1428.

[2] a) A. Mattevi, M. Rizzi, M. Bolognesi, *Curr. Opin. Struct. Biol.* **1996**, *6*, 762–769; b) J. Goldberg, A. C. Nairn, J. Kuriyan, *Cell* **1996**, *84*, 875–887; c) B. Kobe, B. E. Kemp, *Nature* **1999**, *402*, 373–376; d) G. Licini, P. Scrimin, *Angew. Chem.* **2003**, *115*, 4720–4723; *Angew. Chem. Int. Ed.* **2003**, *42*, 4572–4575; e) W. A. Lim, *Curr. Opin. Struct. Biol.* **2002**, *12*, 61–68; f) J. A. Hardy, J. A. Wells, *Curr. Opin. Struct. Biol.* **2004**, *14*, 706–715.

[3] For reviews on synthetic allosteric receptor systems, see: a) T. Nabeshima, *Coord. Chem. Rev.* **1996**, 151–169; b) S. Shinkai, M. Ikeda, A. Sugasaki, M. Takeuchi, *Acc. Chem. Res.* **2001**, *34*, 494–503; c) M. Takeuchi, M. Ikeda, A. Sugasaki, S. Shinkai, *Acc. Chem. Res.* **2001**, *34*, 865–873; d) L. Kovbasyuk, R. Krämer, *Chem. Rev.* **2004**, *104*, 3161–3187; e) S. Shinkai, M. Takeuchi, *Bull. Chem. Soc. Jpn.* **2005**, *78*, 40–51.

[4] a) *Molecular Catenanes, Rotaxanes, and Knots*: *A Journey Through the World of Molecular Topology* (Eds.: J.-P. Sauvage, C. Dietrich-Buchecker), Wiley-VCH, Weinheim, **1999**; b) V. Balzani, A. Credi, F. M. Raymo, J. F. Stoddart, *Angew. Chem.* **2000**, *112*, 3484–3530; *Angew. Chem. Int. Ed.* **2000**, *39*, 3348–3391; c) V. Balzani, M. Venturi, A. Credi, *Molecular Devices and Machines—A Journey into the Nanoworld*, Wiley-VCH, Weinheim, **2003**; d) A. H. Flood, R. J. A. Ramirez, W.-Q. Deng, R. P. Muller, W. A. Goddard, J. F. Stoddart, *Aust. J. Chem.* **2004**, *57*, 301–322; e) "Synthetic Molecular Machines": E. R. Kay, D. A. Leigh in *Functional Artificial Receptors* (Eds.: T. Schrader, A. D. Hamilton), Wiley-VCH, Weinheim, **2005**, pp. 333–406.

[5] For examples of Cu^{II} and Cd^{II} bound to BPA tertiary amide ligands, including several with a central carboxamide nitrogen and discussions of the thermodynamics and kinetics of these coordination modes, see: a) C. Cox, D. Ferraris, N. N. Murthy, T. Lectka, *J. Am. Chem. Soc.* **1996**, *118*, 5332–5333; b) N. Niklas, F. Hampel, G. Liehr, A. Zahl, R. Alsfasser, *Chem. Eur. J.* **2001**, *7*, 5135–5142; c) N. Niklas, F. W. Heinemann, F. Hampel, R. Alsfasser, *Angew. Chem.* **2002**, *114*, 3535–3537; *Angew. Chem. Int. Ed.* **2002**, *41*, 3386–3388; d) N. Niklas, F. W. Heinemann, F. Hampel, T. Clark, R. Alsfasser, *Inorg. Chem.* **2004**, *43*, 4663–4673; e) S. Novokmet, F. W. Heinemann, A. Zahl, R. Alsfasser, *Inorg. Chem.* **2005**, *44*, 4796–4805; f) D. S. Marlin, D. González Cabrera, D. A. Leigh, A. M. Z. Slawin, *Angew. Chem.* **2006**, *118*, 83–89; *Angew. Chem. Int. Ed.* **2006**, *45*, 77–83.

[6] F. G. Gatti, D. A. Leigh, S. A. Nepogodiev, A. M. Z. Slawin, S. J. Teat, J. K. Y. Wong, *J. Am. Chem. Soc.* **2001**, *123*, 5983–5989.

[7] There was no indication of reaction by color change, mass spectrometry, or thin-layer chromatography.

[8] Crystals of **1**$CuCl_2$ and **2**$(CuCl_2)_2$ of suitable quality for X-ray diffraction studies were obtained by carefully layering a solution of the appropriate complex in *N*,*N*-dimethylformamide (DMF) with CH_3CN (approximately 1:10 v/v). Single crystals of **3**, **4**, **5**, and **5**$CuCl_2$ were grown from slow evaporation of saturated solutions in CH_3CN, $CHCl_3$, CH_2Cl_2, and CH_2Cl_2/DMF (5:1 v/v), respectively. Data for **1**$CuCl_2$, **2**$(CuCl_2)_2$, **3**, **4**, and **5**$CuCl_2$ were collected on a Bruker SMART CCD diffractometer, whereas data for **5** were collected on a Rigaku Saturn (MM007 high flux RA/$Mo_{K\alpha}$ radiation, confocal optic). Data were collected at 150 K for **1**$CuCl_2$, **2**$(CuCl_2)_2$, and and **4**, at 125 K for **3** and **5**$CuCl_2$, and at 93 K for **5**. All data collections employed narrow frames (0.3–1.0°) to obtain at least a full hemisphere of data. Intensities were corrected for Lorentz polarization and absorption effects (multiple equivalent reflections). Structures were solved by direct methods, non-hydrogen atoms were refined anisotropically with CH protons being refined in riding geometries (SHELXTL) against F^2. In most cases, amide protons were refined isotropically subject to a distant constraint. Data for **1**$CuCl_2$·3.75 DMF: $C_{73.75}H_{83.75}N_{12.25}O_{9.25}Cl_2Cu$, $M_r = 1424.22$, crystal size $2.07 \times 0.37 \times 0.35\ mm^3$, monoclinic, $P21/c$, $a = 15.5009(8)$, $b = 43.623(2)$, $c = 23.9057(11)$ Å, $Z = 8$, $\rho_{calcd} = 1.231\ Mg\,m^{-3}$; $\mu = 0.415\ mm^{-1}$, 92715 reflections collected, 27020 unique ($R_{int} = 0.0521$) giving $R = 0.0702$ for 18444 observed data [$F_o > 4\sigma(F_o)$], $S = 0.994$ for 1481 parameters; residual electron density extremes were 0.549 and $-0.566\ eÅ^{-3}$. Data for **2**$(CuCl_2)_2$: $C_{70}H_{78}Cl_4Cu_2N_{14}O_8$, $M_r = 1512.34$, crystal size $0.19 \times 0.18 \times 0.08\ mm^3$, monoclinic, $P21/c$, $a = 12.7343(5)$, $b = 19.0061(8)$, $c = 15.7470(7)$ Å, $Z = 2$, $\rho_{calcd} = 1.438\ Mg\,m^{-3}$; $\mu = 0.828\ mm^{-1}$, 20841 reflections collected, 7515 unique ($R_{int} = 0.0450$) giving $R = 0.0791$ for 5367 observed data [$Fo > 4\sigma(F_o)$], $S = 1.112$ for 444 parameters; residual electron density extremes were 0.663 and $-0.851\ eÅ^{-3}$. Data for **3**: $C_{62}H_{56}N_8O_6$, $M_r = 1009.15$, crystal size $0.21 \times 0.1 \times 0.1\ mm^3$, monoclinic, $C2/c$, $a = 31.107(10)$, $b = 18.677(6)$, $c = 21.001(7)$ Å, $Z = 8$, $\rho_{calcd} = 1.318\ Mg\,m^{-3}$; $\mu = 0.086\ mm^{-1}$, 31645 reflections collected, 9198 unique ($R_{int} = 0.5301$) giving $R = 0.1611$ for 2791 observed data [$F_o > 4\sigma(F_o)$], $S = 0.994$ for 707 parameters; residual electron density extremes were 0.383 and $-0.380\ eÅ^{-3}$. Data for **4**·$(CHCl_3)_3$: $C_{64}H_{58}Cl_{12}N_{10}O_6$, $M_r = 1488.66$, crystal size $0.59 \times 0.46 \times 0.41\ mm^3$, triclinic, $P\bar{1}$, $a = 11.8069(7)$, $b = 12.2006(7)$ Å, $Z = 4$, $\rho_{calcd} = 1.485\ Mg\,m^{-3}$; $\mu = 0.559\ mm^{-1}$, 16004 reflections collected, 7684 unique ($R_{int} = 0.04$) giving $R = 0.0526$ for 6362 observed data [$F_o > 4\sigma(F_o)$], $S = 0.9917$ for 415 parameters; residual electron density extremes were 0.44 and $-0.36\ eÅ^{-3}$. Data for **5**: $C_{62}H_{59}N_9O_8$, $M_r = 1058.18$, crystal size $0.1 \times 0.03 \times 0.03\ mm^3$, triclinic, $P\bar{1}$, $a = 10.9491(5)$, $b = 14.8382(2)$, $c = 18.5719(8)$ Å, $Z = 2$, $\rho_{calcd} = 1.311\ Mg\,m^{-3}$; $\mu = 0.716\ mm^{-1}$, 32650 reflections collected, 7414 unique ($R_{int} = 0.0782$) giving $R = 0.0806$ for 5270 observed data [$F_o > 4\sigma(F_o)$], $S = 1.051$ for 746 parameters; residual electron density extremes were 0.288 and $-0.313\ eÅ^{-3}$. Data for **5**$CuCl_2$·3 DMF·2 H_2O: $C_{68.75}H_{75.75}Cl_2CuN_{11.25}O_{10.75}$, $M_r = 1366.1$, crystal size $0.16 \times 0.1 \times 0.1\ mm^3$, monoclinic, $P2(1)/n$, $a = 25.279(6)$, $b = 10.970(3)$, $c = 25.649(6)$ Å, $Z = 4$, $\rho_{calcd} = 1.288\ Mg\,m^{-3}$; $\mu = 0.451\ mm^{-1}$, 44451 reflections collected, 12876 unique ($R_{int} = 0.4536$) giving $R = 0.1614$ for 4795 observed data [$F_o > 4\sigma(F_o)$], $S = 1.038$ for 856 parameters; residual electron density extremes were 1.180 and $-0.718\ eÅ^{-3}$. The protons on solvate molecules were not allowed for in the refinement. CCDC 281563–281568 (**1**$CuCl_2$, **2**$(CuCl_2)_2$,

3, **4**, **5**, and **5**$CuCl_2$, respectively) contain the supplementary crystallographic data for this paper. These data can be obtained free of charge from The Cambridge Crystallographic Data Centre via www.ccdc.cam.ac.uk/data_request/cif.

[9] A. Altieri, G. Bottari, F. Dehez, D. A. Leigh, J. K. Y. Wong, F. Zerbetto, *Angew. Chem.* **2003**, *115*, 2398 – 2402; *Angew. Chem. Int. Ed.* **2003**, *42*, 2296 – 2300.

[10] For other examples of negative heterotropic allostery in artificial systems, see: a) M. H. Al-Sayah, N. R. Branda, *Angew. Chem.* **2000**, *112*, 975 – 977; *Angew. Chem. Int. Ed.* **2000**, *39*, 945 – 947; b) M. H. Al-Sayah, N. R. Branda, *Chem. Commun.* **2002**, 178 – 179; c) P. Thordarson, E. J. A. Bijsterveld, J. A. A. W. Elemans, P. Kasak, R. J. M. Nolte, A. E. Rowan, *J. Am. Chem. Soc.* **2003**, *125*, 1186 – 1187; d) M. H. Al-Sayah, R. McDonald, N. R. Branda, *Eur. J. Org. Chem.* **2004**, 173 – 182.

[11] A. H. Flood, J. F. Stoddart, D. W. Steuerman, J. R. Heath, *Science* **2004**, *306*, 2055 – 2056.

[12] G. Bottari, D. A. Leigh, E. M. Pérez, *J. Am. Chem. Soc.* **2003**, *125*, 13360 – 13361.

[13] a) Q.-C. Wang, D.-H. Qu, J. Ren, K. Chen, H. Tian, *Angew. Chem.* **2004**, *116*, 2715 – 2719; *Angew. Chem. Int. Ed.* **2004**, *43*, 2661 – 2665; b) D.-H. Qu, Q.-C. Wang, J. Ren, H. Tian, *Org. Lett.* **2004**, *6*, 2085 – 2088; c) E. M. Pérez, D. T. F. Dryden, D. A. Leigh, G. Teobaldi, F. Zerbetto, *J. Am. Chem. Soc.* **2004**, *126*, 12210 – 12211; d) D. A. Leigh, M. Á. F. Morales, E. M. Pérez, J. K. Y. Wong, C. G. Saiz, A. M. Z. Slawin, A. J. Carmichael, D. M. Haddleton, A. M. Brouwer, W. J. Buma, G. W. H. Wurpel, S. León, F. Zerbetto, *Angew. Chem.* **2005**, *117*, 3122 – 3127; *Angew. Chem. Int. Ed.* **2005**, *44*, 3062 – 3067.

[14] T. D. Nguyen, H.-R. Tseng, P. C. Celestre, A. H. Flood, Y. Liu, J. F. Stoddart, J. I. Zink, *Proc. Natl. Acad. Sci. USA* **2005**,*102*, 10029 – 10034.

[15] J. Berná, D. A. Leigh, M. Lubomska, S. M. Mendoza, E. M. Pérez, P. Rudolf, G. Teobaldi, F. Zerbetto, *Nat. Mater.* **2005**, *4*, 704 – 710.

[16] Y. Liu, A. H. Flood, P. A. Bonvallet, S. A. Vignon, B. H. Northrop, H.-R. Tseng, J. O. Jeppesen, T. J. Huang, B. Brough, M. Baller, S. Magonov, S. D. Solares, W. A. Goddard, C.-M. Ho, J. F. Stoddart, *J. Am. Chem. Soc.* **2005**, *127*, 9745 – 9759.

